Cellulose
https://doi.org/10.1007/s10570-023-05495-z

ORIGINAL RESEARCH

Design of cellulose nanofibre-based composites with high barrier properties

Luís Alves · Ana Ramos · Eduardo Ferraz · Paulo J. T. Ferreira · Maria G. Rasteiro · José A. F. Gamelas

Received: 17 March 2023 / Accepted: 2 September 2023

Abstract Gas barrier properties are very relevant in composite materials for applications so diverse such as food packaging, electronics, or old document restoration. In the present work, four different types of cellulose nanofibres (CNFs), two types of clay minerals used individually (sepiolite) or combined (sepiolite + kaolinite), and the influence of pH, were explored in the production of composite films. Neat CNFs, only mechanically treated or prepared by enzymatic pretreatment, gave films with good mechanical and barrier properties, but the addition of minerals led to a dramatic loss of these properties. Contrarily, the use of thin and functionalized fibrils (TEMPO-oxidised or cationized CNFs) gave composite films with good mechanical, thermal and barrier properties. Superior oxygen barrier properties (oxygen transmission rate (OTR) < 0.4 cm^3 m^{-2} day^{-1}) were obtained using TEMPO-oxidised CNF and 20% sepiolite, and, in general, for all the composite films containing the TEMPO CNF (OTR ≤ 1.8 cm^3 m^{-2} day^{-1}). The cationic CNF-based composites also showed a very good oxygen barrier (OTR ≤ 8.2 cm^3 m^{-2} day^{-1}). The high oxygen barrier could be explained by the compactness of the films and better entanglement of the more fibrillated nanocelluloses with the mineral particles. A decrease in the pH of the suspensions led to a decrease in the film preparation time, without a major negative impact on the composite film's properties.

Keywords Nanocellulose · Cellulose nanofibrils · Water vapour transmission rate · Oxygen transmission rate · Gas permeability · Tensile strength

Supplementary Information The online version contains supplementary material available at https://doi.org/10.1007/s10570-023-05495-z.

L. Alves (✉) · P. J. T. Ferreira · M. G. Rasteiro · J. A. F. Gamelas (✉)
Department of Chemical Engineering, CIEPQPF, University of Coimbra, Rua Sílvio Lima, Pólo II, 3030-790 Coimbra, Portugal
e-mail: luisalves@ci.uc.pt

J. A. F. Gamelas
e-mail: jafgas@eq.uc.pt

A. Ramos
Department of Chemistry, FibEnTech, University of Beira Interior, Rua Marquês d'Ávila e Bolama, 6201-001 Covilhã, Portugal

E. Ferraz
Techn&Art, Polytechnic Institute of Tomar, Quinta do Contador, Estrada da Serra, 2300-313 Tomar, Portugal

E. Ferraz
Geosciences Department, Geobiotec, University of Aveiro, Campus Universitário de Santiago, 3810-193 Aveiro, Portugal

Introduction

In recent years, a lot of scientific research has been devoted to developing materials with lower environmental impact, suitable to substitute plastics in

Published online: 20 September 2023

different applications. It is known that plastics, microplastics, and nanoplastics are spread in terrestrial and aquatic media, with severe problems for terrestrial and aquatic life, being a large contribution for that given by the single-use plastics employed, for instance, in food packaging (Abbasi et al. 2018; Hale et al. 2020; Magalhães et al. 2020). Cellulose-based materials are obvious candidates due to the wide abundance and excellent properties of this biomaterial (Alves et al. 2019). However, so far, the cellulose-based materials developed to substitute plastics in food packaging have shown some limitations, mainly related to the poor gas barrier properties (Wang et al. 2018), under high moisture conditions. The water vapour and oxygen barriers are key properties in food packaging because the quality of the food and the shelf life is greatly influenced by the properties of the packaging.

Among the available cellulose-based materials, cellulose nanofibres (CNFs) are regarded as materials with great potential for applications such as food packaging. These nanomaterials present desirable properties, which include high biocompatibility and biodegradability, superior film-forming capability, and good mechanical properties (Zeng et al. 2021). However, driven by the high energy consumption and/or pre-treatments needed for their preparation, CNFs are still relatively expensive nanomaterials, this being one of the main drawbacks related to the replacement of plastic materials with nanocellulose-based ones. Strategies have been developed to reduce costs, without compromising the properties of the developed materials, and even improving for example the barrier properties. One of the most promising approaches involves the preparation of CNF-mineral nanocomposites (Alves et al. 2019; Gamelas and Ferraz 2015; González del Campo et al. 2018). A quick look at the available literature reveals that most of the studies reporting CNF-mineral composites were developed using planar minerals, such as montmorillonite, vermiculite or saponite (Alves et al. 2019). Only a minor number of works were developed using other types of minerals, such as fibrous clay minerals.

Sepiolite (SEP) is a fibrous clay, available in nature, composed of highly porous frameworks derived from the presence of cavities (tunnels), being the ideal formula $Mg_8Si_{12}O_{30}(OH)_4(OH_2)_4.8H_2O$. An important characteristic of this mineral is the high density of silanol groups on the particle surface, allowing the interaction of the mineral with the other composite components by hydrogen bonding. Moreover, other interactions, such as Van der Waals interactions, contribute to the presence of aggregates of the acicular individual particles of this fibrous clay, reducing the dispersibility of the individual particles in the prepared suspensions (Wang and Wang 2019), and thus impacting the properties of the prepared composites, very dependent on the dispersion state and mixture of the different components (Alves et al. 2019).

Several strategies can be employed to improve the dispersion stability of sepiolite and positively impact the properties of the prepared composites (Alves et al. 2020b). González del Campo et al. (2020) reported the use of ultrasound irradiation to prepare nanocomposite materials by assembling fibrous clays and cellulose nanofibres. The obtained films presented good mechanical properties (Young's modulus of 2.8 GPa) and reasonable water vapour barrier properties (water vapour transmission rate (WVTR) of 286 g m^{-2} day^{-1}) with the optimal loading of 20% of sepiolite, being the barrier properties highly affected by an increase of the mineral content. The same strategy was also used to prepare CNF-sepiolite composite films and modify those films with magnetite and ZnO nanoparticles, for applications in biomedical and biotechnological fields (González del Campo et al. 2018).

Very recently, Martín-Sampedro et al. (2022) also used ultrasonication and Ultra-Turrax homogenizer to prepare mixtures of sepiolite and nanocelluloses able to form nanopapers. The authors stated that the properties, such as flammability, water vapour permeability, and mechanical and optical properties of the obtained nanopapers would be dependent on the type of nanocellulose and the sepiolite content. They reported a worsening of the barrier properties with the increment of the sepiolite content.

On the other hand, Ghanadpour et al. (2018a) prepared thin films, based on phosphorylated cellulose nanofibres and sepiolite, with flame retardancy, to coat polyethylene. The prepared CNF-sepiolite films were not able to entirely prevent the ignition of the film-coated polyethylene composite, contrary to the films prepared with montmorillonite, which could create an excellent barrier and thermal shielding, probably due to its lamellar structure. However, in another work, Köklükaya et al. (2020) reported

that the incorporation of sepiolite in a layer-by-layer coating of cellulose fibres allowed for good fire retardancy properties, even compared with the use of montmorillonite. Likewise, Gupta et al. (2019) prepared sepiolite-based aerogels, with flame retardancy and thermal insulation properties, stabilized by cellulose nanofibrils, to be used in buildings. Ghanadpour et al. (2018b) also prepared nanocomposite foams using phosphorylated nanocellulose with excellent flame-retardant properties and self-extinguishing behaviour. The retardancy properties were attributed mainly to the intrinsic charring ability of the phosphorylated fibrils, and the capability of sepiolite to form an intumescent-like barrier on the surface of the material.

Sanguanwong et al. (2021) modified the surface of CNF-sepiolite foams with methyltrimethoxysilane to produce hydrophobic composites, with good oil sorption capacity and good mechanical properties. A different approach was used by Lisuzzo et al. (2020) who assembled two distinct minerals with cellulose nanofibrils to produce functional biohybrid materials. The mixture of nanotubular halloysite and microfibrous sepiolite allowed for the preparation of homogeneous, flexible, and strong films, with the capacity to load and release model drugs.

On the other hand, kaolinite is an abundant clay with platelet-like morphology and ideal formula $Al_2Si_2O_5(OH)_4$, which can have a high aspect ratio (diameter to thickness ratio) (Castro et al. 2018). In the few works found of CNF-kaolinite composites, Honorato et al. (2015) compared the use of kaolinite with $CaCO_3$ to prepare TEMPO-oxidised CNF composites. The use of the clay provided better results, regarding the film properties, having been obtained highly brittle composite films with $CaCO_3$. In a different approach, Castro et al. (2018) used a pilot paper machine to scale-up nanocomposites based on cellulose fibres, microfibrillated cellulose and kaolinite with fire retardancy properties. The addition of kaolinite led to a reduction in the mechanical properties (tensile strength and Young's modulus) and a large increase in the porosity of the material with microfibrillated cellulose, which was attributed to a poor interfacial adhesion between kaolinite and microfibrillated cellulose. Spence et al. (2011) reported a decrease in the WVTR of microfibrillated cellulose composite films with the addition of kaolinite, being that decrease attributed to an increase in the tortuosity of the composite matrix.

In the present work, it was hypothesized that the type of CNFs used, the film formulation, as well as the film compactness, have a deep impact on the properties of the produced films, mainly on their barrier properties. To infer this hypothesis, four different types of cellulose nanofibrils (produced by only mechanical treatment, pre-treated with enzyme, pre-treated by TEMPO mediated oxidation, and pre-treated by cationization with (3-chloro-2-hydroxypropyl)trimethylammonium chloride), as well as the use of a single clay mineral (sepiolite), or the combination of two different clay minerals (sepiolite + kaolinite), were explored to understand the effect on the properties of CNF-based composite films. Fibrous minerals have been less explored to prepare composite films with CNFs, and, from the best of our knowledge, no work has reported the effect of some CNF types, such as enzymatic or cationic, on the properties of composite films with fibrous minerals. Also, not found in the literature is the effect of the combination of sepiolite and kaolinite on the performance of CNF-based composites. Additionally, the effect of the suspension pH used to prepare the composites was also evaluated. The optical, mechanical, thermal, and gas barrier properties of the prepared composite films were determined, for the different film compositions, comprising variations of the CNF type, type of mineral (single or a combination), and suspension pH, at a fixed mineral load of 20%.

Materials and methods

Materials

Bleached *Eucalyptus globulus* kraft pulp supplied by the Navigator Company was used for the preparation of all types of CNFs. The sepiolite sample was supplied by Tolsa, SA (Spain) and kaolin was purchased from Imerys Minerals (UK). Carboxymethylcellulose sodium salt with a molecular weight of 250 kDa and a degree of substitution of 0.7, (3-chloro-2-hydroxypropyl)trimethylammonium chloride (CHPTAC) 60 wt.% aqueous solution, sodium hydroxide (≥ 98%, pellets), 2,2,6,6-Tetramethylpiperidine 1-oxyl (TEMPO radical, ≥ 98%), and sodium bromide were obtained from Sigma-Aldrich (Merck). Sodium hypochlorite

with 14% active chlorine was purchased from VWR Chemicals.

Preparation of CNFs and mineral suspensions

In the present study, four different cellulose nanofibre types were used, namely Mec CNF (prepared using only mechanical treatments), Enz CNF (obtained by pre-treatment with an enzyme before high-pressure homogenization), T55 CNF (pre-treated with sodium hypochlorite in the presence of TEMPO radical followed by high-pressure homogenization), and Cat CNF (pre-treated with CHPTAC previous to high-pressure homogenization). The different CNFs were obtained and characterized following previously described procedures (Alves et al. 2022; Pedrosa et al. 2022). For the Cat CNF, a NaOH/anhydroglucose molar ratio of 2 and CHPTAC/anhydroglucose molar ratio of 0.5 were used, and the cationization occurred for 4 h at 70 °C. Suspensions ranging from 0.71 to 0.94 wt.% (dry basis) of CNFs were obtained, after the high-pressure homogenization step, and used to prepare the neat CNF and composite films. The most relevant characterization data of the produced CNFs are shown in Table S1. Two different clay minerals were also used in the present work: a high purity (> 95%) sepiolite sample from the deposit of Vallecas-Vicálvaro (Madrid, Spain), which had been previously processed by dry micronization into micron-size particles (Alves et al. 2020b) and a kaolin (Super Standard Porcelain) composed by ca. 90% of kaolinite mineral.

Sepiolite aqueous suspensions at 1.0 wt.% were prepared, previously to film preparation, using a Dispermat CV3-PLUS-E high-shear disperser at 5000 rpm for 15 min (Alves et al. 2022). Suspensions of 1.0 wt.% kaolinite were also prepared, using as dispersing agent, carboxymethylcellulose, and as dispersing equipment an ultrasonic probe (Vibra-cell VC 505, Sonics, Newtown, CT, USA) for 10 min, working at 60% amplitude and 1 s pulse (Ferraz et al. 2021).

Preparation of the neat CNF films and CNF-mineral composite films

Films with different compositions, with only CNFs and CNF-mineral composite films, were prepared using the approach of filtration followed by hot pressing, according to a previously described procedure (Alves et al. 2022). Films were designed to have a grammage of 40 g m^{-2} and 20% mineral content in the case of the composites. In brief, the different formulations, consisting only of CNFs (Mec, Enz, T55, and Cat), mixtures of CNFs with sepiolite, and mixtures of CNFs with kaolinite and sepiolite, were diluted to obtain aqueous suspensions containing ca. 0.2 wt.% solid content (dry basis). Next, the suspensions were allowed to disperse for 10 min at 1000 rpm using the Dispermat high-shear disperser. The obtained dispersed suspensions were dewatered using a filtration unit from Kimble Ultra-Ware Filtration Systems (DWK Life Sciences GmbH, Mainz, Germany) and cellulose acetate membranes with 0.45 µm pore and 90 mm diameter (Filtratech, France). The "wet cakes", retained over the membranes, were finally dried using a rapid dryer for laboratory sheets (Lorentzen & Wettre, model 257, Lorentzen & Wettre GmbH, Munich, Germany) for 10 min at 110 °C. The obtained films were stored for further characterization. A list of the produced films with their composition is shown in Table 1.

Characterization of the CNF-based films

The obtained films were characterized in terms of optical, mechanical and barrier properties, as well as for the thermal properties (thermogravimetry), morphology (scanning electron microscopy) and by

Table 1 The prepared CNF-clay composite films and neat CNF films

Film composition	Mec CNF	Enz CNF	T55 CNF	Cat CNF
Neat CNF (100%)	✓	✓	✓	✓
80% CNF + 20% SEP	✓	✓	✓	✓
80% CNF + 10% SEP + 10% Kao	✓	✓	✓	✓
80% CNF + 20% SEP, pH 3	✓	✓	✓	–
80% CNF + 10% SEP + 10% Kao, pH 3	✓	✓	✓	–

FTIR. The optical properties (transparency) were accessed according to the ISO 22891 standard, using a Technidyne Color Touch 2 spectrophotometer (Technidyne Corporation, New Albany, Indiana, USA). Two film replicates were analysed for each formulation, by applying the illuminant D65 and the observer 10º. The thickness of the different films was measured using a micrometre (Adamel Lhomargy, model MI 20, Roissy-en-Brie, France), based on ten measurements for two replicates, being reported the average value obtained for these measurements. The tensile properties were determined according to the ISO 1924–1 standard, at 23 ± 1 °C and 50 ± 2% RH, using a tensile tester (Thwing-Albert Instrument Co., EJA series, West Berlin, NJ, USA). The following setup of the tensile tester was used to study the tensile properties: a tensile rate of 5 mm per minute and an initial gap between grips of 5 cm. The properties studied were the tensile strength, Young's modulus and elongation at break, and the reported values correspond to the average of four specimens for each film type.

The morphology of the surface and the cross-section (after cryofracture) of the different films were examined using a field emission Carl Zeiss Merlin microscope (Carl-Zeiss, Germany), in secondary electron mode. An acceleration voltage of 2 kV and a working distance of 6 mm was used to obtain the images of the gold sputter-coated samples. The homogeneity and microstructure of the films were studied for the different film formulations.

FTIR-ATR spectra of the films were recorded in a JASCO FT/IR-4200 spectrometer (Jasco Corporation, Tokyio, Japan) using a universal ATR accessory, in the range of 500–4000 cm^{-1}, with a resolution of 4 cm^{-1} and applying 128 scans.

Thermal analysis was performed using a SDT Q600 thermal analyser from TA instruments. The samples were heated under a nitrogen flow (100 mL min^{-1}) from room temperature up to 1000 °C, at a rate of 10 °C min^{-1}. For a better normalization of the values, the char residue was estimated on a dry basis of material, that is, using the weight obtained after the thermogravimetric loss (at 150 °C) due to moisture and adsorbed water.

The water vapour transmission rate (WVTR) and water vapour permeability (WVP) were evaluated by the gravimetric method according to the ASTM E96-00 standard. WVTR (in g m^{-2} day^{-1}) and WVP (in g Pa^{-1} day^{-1} m^{-1}) were obtained at 23 ± 1 °C and 50 ± 2% RH. The mass changes (Δm) were measured every hour for 48 h. The WVTR was calculated by the ratio between the slope of the straight line (Δm/Δt) and the exposed film area (in m^2). WVP was obtained from the WVTR value, as previously detailed (Almeida et al. 2021).

The oxygen transmission rate (OTR) of the films was measured using a Mocon Ox-Tran 2/22 equipment in accordance with ASTM F1927-20. The measurements were carried out under similar temperature and RH conditions of the WVTR measurements. The oxygen permeability (OP) was calculated from the OTR, by multiplying it by the film thickness.

Results and discussion

Characterization of the CNF-based composite films

Electron microscopy studies

The microstructure of the composite films prepared was firstly studied by scanning electron microscopy. The images obtained for the different materials are depicted in Fig. 1 (films of the CNFs with the lowest and highest degree of fibrillation, as examples).

In general, all the prepared films appeared in an oriented layered structure, without evident signs of clay and CNF segregation. The present observations are in line with previous works, in which films prepared by filtration followed by hot pressing presented well-defined layers of oriented particles (Alves et al. 2022). The absence of segregation between the CNFs and minerals could explain the good performance of the composite films, mainly the ones prepared using T55 and Cat CNFs, as shown below in "Optical properties of the CNF-based composite films, Mechanical properties of the CNF-based composite films and Barrier properties of the CNF-based composite films" sections. On the other hand, changing the pH of the film preparation also did not result in relevant changes in the layered structure of the films, even though some aggregation of fibrils could be induced previously to film formation (Alves et al. 2020a).

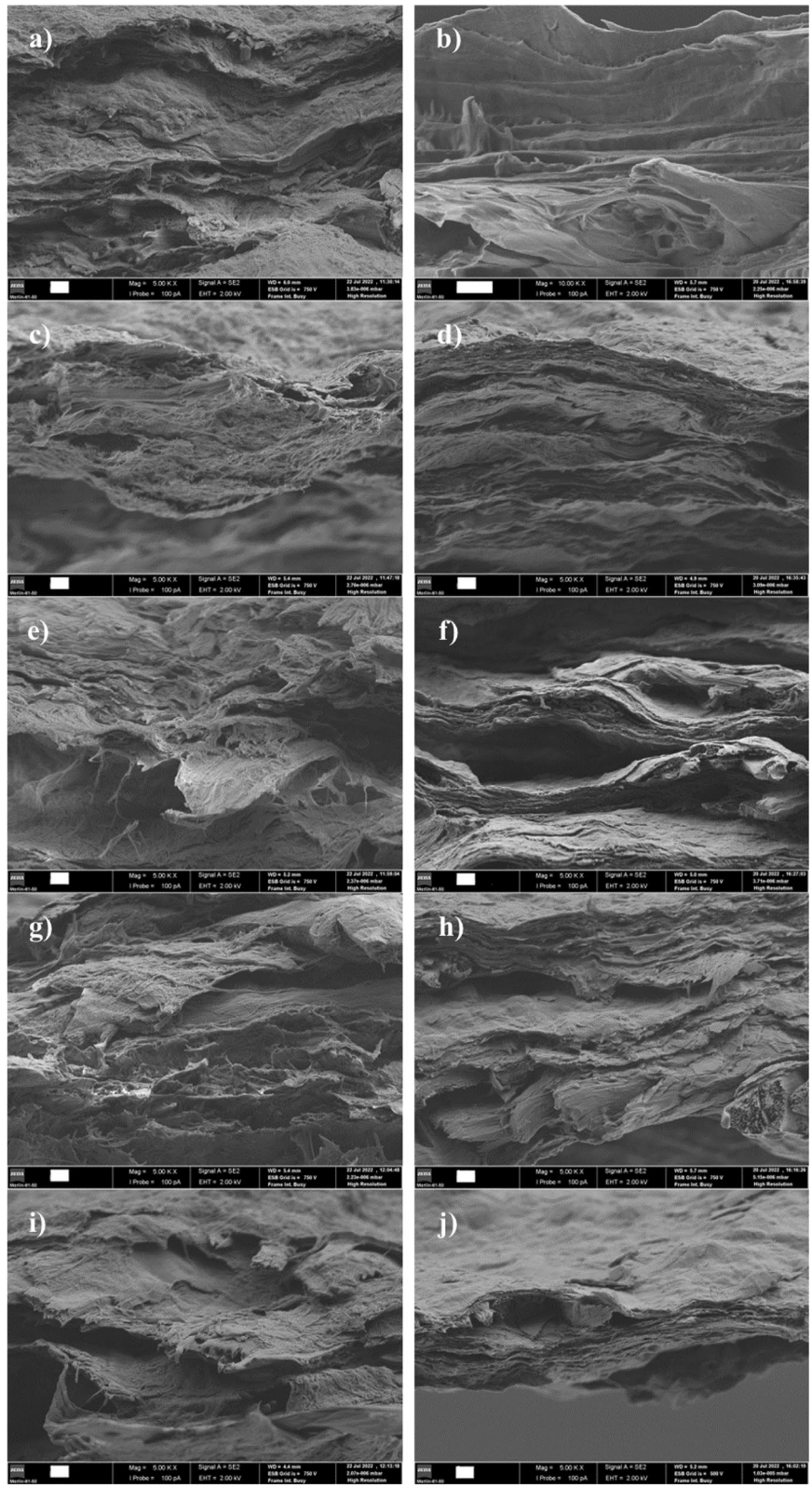

Fig. 1 Scanning electron microscopy images of CNF-based composite films at a magnification of 5000x. **a** Mec CNF; **b** T55 CNF; **c** Mec CNF + 20% sepiolite; **d** T55 CNF + 20% sepiolite; **e** Mec CNF + 20% sepiolite pH 3; **f** T55 CNF + 20% sepiolite pH 3; **g** Mec CNF + 10% sepiolite + 10% kaolinite; **h** T55 CNF + 10% sepiolite + 10% kaolinite; **i** Mec CNF + 10% sepiolite + 10% kaolinite pH 3; **j** T55 CNF + 10% sepiolite + 10% kaolinite pH 3. The scale bars represent 1 µm

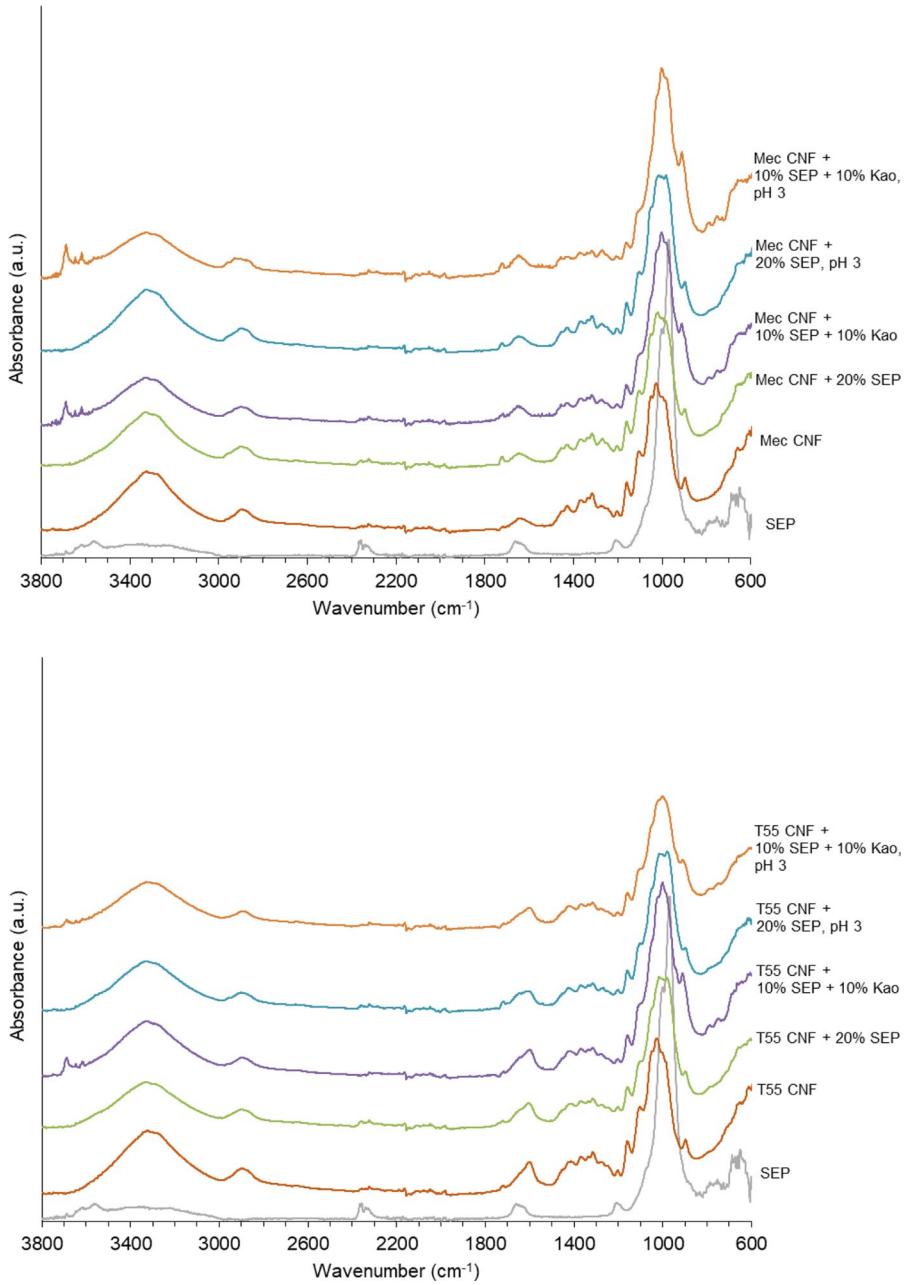

Fig. 2 FTIR spectra of series of films of Mec CNF and T55 CNF with minerals

FTIR studies

The films were also analysed by FTIR spectroscopy. The infrared spectra of the different CNF film series are presented in Fig. 2 (series of Mec CNF and TEMPO CNF) and Figure S1 (series of Enz CNF and Cat CNF). The infrared data of the films of only CNFs showed the prevalence of the characteristic bands of cellulose; namely, bands at ca. 897, 1103 and 1160 cm^{-1} were observed, due to C1–H bending and C–O stretching vibration modes. Additionally, the highest absorption was observed in the region of 1000–1050 cm^{-1}, with maxima at 1027 cm^{-1}. For the T55 CNF film, a strong band at ca. 1600 cm^{-1} appeared, indicating the presence of carboxylate groups from the TEMPO-mediated oxidation (COO^- asymmetric stretching). This band prevailed

over the band at ca. 1645 cm^{-1} from the O–H bending of adsorbed water.

With the sepiolite incorporation (20%) in the films, some changes were evident in the absorption spectra. In the region from 800 to 1100 cm^{-1}, the envelope of the strongest band and the position of the maximum changed slightly, reflecting the presence of sepiolite which has a strong absorption (Si–O stretching) at ca. 970 cm^{-1} (Fig. 2), for which bands overlapped with the characteristic absorption of cellulose. Typically, a maximum at 1015–1020 cm^{-1} was observed. The 897 cm^{-1} band was also reduced in intensity reflecting the presence of sepiolite. FTIR spectroscopy did not enable to assess the chemical interactions between the sepiolite and CNF in the composite films, as the vibration bands of CNF attenuated and masked the sepiolite bands, due to the higher content of CNF (80%) in the films. For instance, the very weak bands for the O–H stretching in the Si–O–H, Mg–O–H and $Mg–OH_2$ bonds of sepiolite were absent in the spectra of the composites (region of 3500–3750 cm^{-1}).

With the additional incorporation of kaolinite (10% sepiolite + 10% kaolinite), the spectra showed further changes in the position of the absorption maximum to 999–1003 cm^{-1} for the different CNFs. Additional bands in the 3600–3700 cm^{-1} region, namely at 3617, 3647 and 3687 cm^{-1}, due to kaolinite (O–H bending), were also observed, which were at similar wavenumber of those observed in the kaolinite-only spectrum.

For the films of CNFs and minerals prepared at pH 3, the FTIR spectra were reasonably similar to those of the corresponding films prepared at near neutral pH, and no further interactions could be deduced from the FTIR data analysis.

Thermogravimetric studies

The thermogravimetric data showed different trends regarding thermal properties depending, mainly, on the type of CNFs evaluated. The main results are summarized in Table 2. The thermograms and the corresponding derivative curves for all the series of composite films are presented in Fig. 3 and Figure S2. The onset temperature for the degradation of the cellulosic component varied according to the film prepared. Neat films of Mec CNF and Enz CNF were more thermally stable (T_{on} of 253–255 °C) than those of T55 CNF and Cat CNF (T_{on} of 203 and 225 °C, respectively). Note that degradation of T55 CNF is

Table 2 Thermogravimetric data of films of CNFs with minerals (basis weight of 40 g m^{-2})

Film	T_{on} (°C)[a]	T_{max} (°C)[b]	Char residue (%)[c]
Mec CNF	253	320	18.8
Mec CNF + 20% SEP	207	350	25.3
Mec CNF + 10% SEP + 10% Kao	218	350	25.2
Mec CNF + 20% SEP, pH 3	228	348	24.7
Mec CNF + 10% SEP + 10% Kao, pH3	231	338	29.3
Enz CNF	255	343	18.8
Enz CNF + 20% SEP	221	345	28.2
Enz CNF + 10% SEP + 10% Kao	243	348	25.9
Enz CNF + 20% SEP, pH 3	246	339	20.0
Enz CNF + 10% SEP + 10% Kao, pH3	253	342	22.5
T55 CNF	203	244/310	22.8
T55 CNF + 20% SEP	203	252/320	39.6
T55 CNF + 10% SEP + 10% Kao	218	266/326	42.1
T55 CNF + 20% SEP, pH 3	212	268(sh)/326	34.8
T55 CNF + 10% SEP + 10% Kao, pH3	217	271(sh)/333	43.9
Cat CNF	225	314/345	17.6
Cat CNF + 20% SEP	231	313/351	32.6
Cat CNF + 10% SEP + 10% Kao	240	315	37.6

[a]Temperature corresponding to the onset of material degradation. Values with an estimated error around 3 °C

[b]Temperature(s) corresponding to the maximum degradation rate (based on derivative curve). Values with an estimated error around 3 °C

[c]Based on final residue at 1000 °C relatively to the mass obtained at 150 °C (dry basis): (mf/m150) × 100. Values with an estimated error around 0.5%

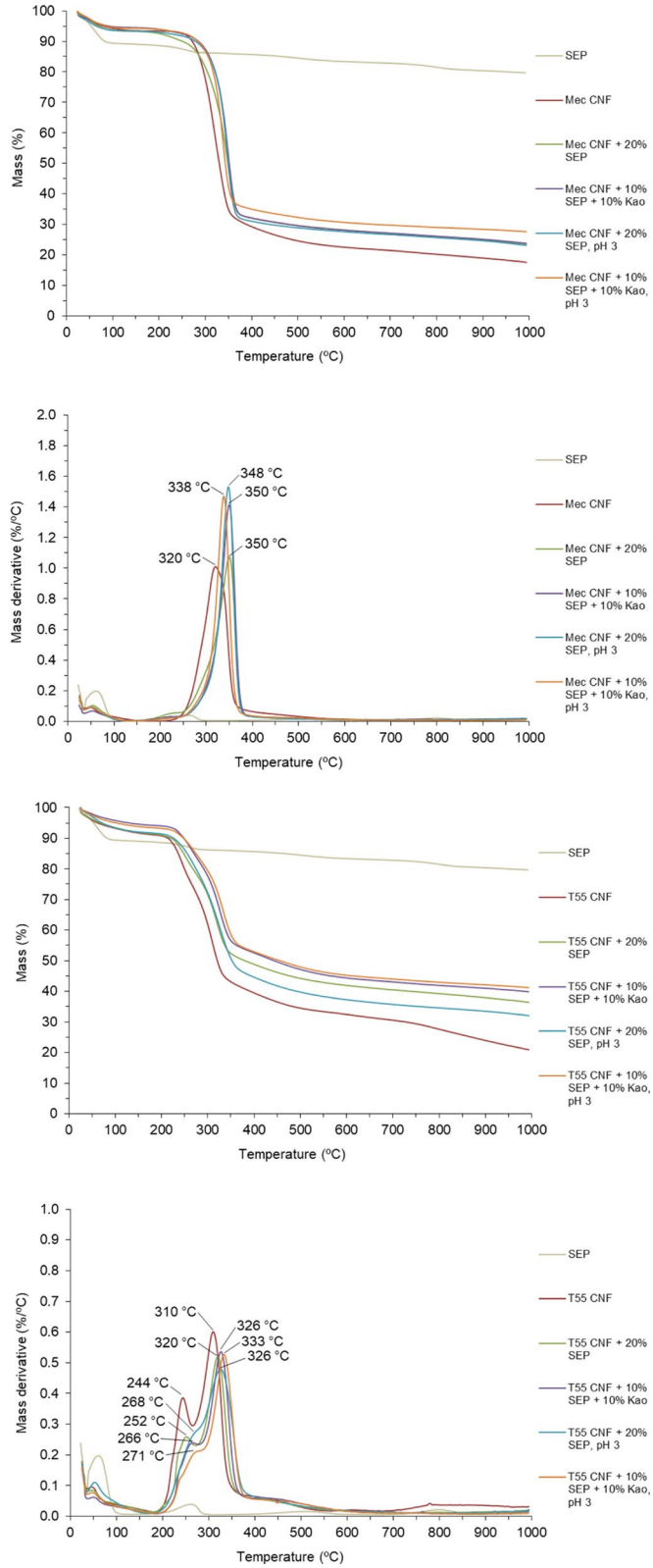

Fig. 3 Thermograms and derivative curves for the Mec CNF and T55 CNF-based composite films

initiated by the decomposition of carboxylic groups that are linked to the glucose units of the cellulose chain. This is the reason why the neat T55 CNF film was less stable than the corresponding films of Mec CNF and Enz CNF. It was also less stable than the neat Cat CNF film, although, for the latter, degradation of substituent alkylammonium groups limits its stability in comparison to Mec CNF and Enz CNF. Depolymerization of cellulose to volatile levoglucosan and formation of aromatic char are considered to be the main steps responsible for cellulose degradation and weight losses observed (Ghanadpour et al. 2018b).

The mineral incorporation in the films had different effects: in the case of the Mec CNF and Enz CNF films, the mineral (sepiolite alone or sepiolite combined with kaolinite) reduced the onset temperature of degradation (lower thermal stability). However, for the T55 CNF and Cat CNF films, there was a general improvement in the thermal stability with the mineral incorporation in the film (20%). Note, as well, that the concomitant introduction of lamellar mineral seemed to improve slightly the thermal stability of the composite films in comparison with the composite films prepared with only CNFs + sepiolite (218 vs. 207 °C for Mec CNF, 243 vs. 221 °C for Enz CNF, 218 vs. 203 °C for T55 CNF, and 240 vs. 231 °C for Cat CNF). When the film preparation was run at pH 3, an improvement in the thermal stability for Mec CNF and Enz CNF was observed (vs. the preparations at near neutral pH). In the case of T55 CNF, a similar improvement was observed for the preparation with only sepiolite at 20% content (212 vs. 203 °C).

Concerning the temperature of maximum degradation rate, T_{max} (Table 2, Fig. 3 and Figure S2), the trends were not the same as those observed for the onset degradation temperature. This temperature was increased for Mec CNF-based films from 320 °C (neat CNF) to 338–350 °C (composites), whereas for Enz CNF, the variations were very small between films ($\leq$5 °C). In the case of the T55 CNF series, two peaks (or a shoulder plus peak) were observed in the derivative curve. Both the peaks were shifted to higher temperatures after sepiolite incorporation, confirming an increment in the thermal stability of the material. Similar to the T_{on} trend, the experiments conducted at pH 3 seemed to promote a slight increment of the T_{max} for T55 CNF + sepiolite films. The same effect was observed for the introduction of the lamellar mineral (kaolinite). For Cat CNF films, two peaks were also observed (except for the case of kaolinite incorporation), like the behaviour of the corresponding T55 CNF-based films, although, compared to the latter their positions differed significantly.

As for the char residue value, there was an increment for the composite films in comparison to the neat CNF films, as it would be expected, since the mineral weight loss in the range of temperature studied is much lower than that of CNFs (Fig. 3 and Figure S2). The highest char residues were obtained for the films of T55 CNF with minerals followed by the films of Cat CNF with minerals. For example, the neat T55 CNF film presented a char (at 1000 °C) of 23% that increased for the film of T55 CNF with 20% sepiolite to 40%. The film with 10% sepiolite and 10% kaolinite had a char of 42%.

It should be highlighted that for the case of a composite film of sepiolite (20%) with T55 CNF, a char of ca. 34% would be predicted by considering the losses observed in the individual thermograms of neat CNF and sepiolite and the proportions of these two components used in the film production, assuming no synergy between the components. However, the amount of char in the composite was significantly higher, showing that the addition of sepiolite besides improving the thermal stability of T55 CNF film, also limited the release of volatile and combustible compounds to lower values during thermal degradation. This is an important result concerning the use of these films as flame-retardant materials.

The present results showed that the improvement in thermal stability of the CNF-sepiolite composites can be conditioned by the type of CNFs used in the formulations. Under the conditions applied for the preparation of the composite films, the mineral (sepiolite or sepiolite + kaolinite) had a positive effect when combined with the more nano-fibrillated T55 and Cat CNFs, but not combined with the more difficult to disperse Mec CNF and Enz CNF nanocelluloses, majorly comprising microfibrillated material. No previous studies are available on films made of sepiolite and nanocellulose pre-treated by enzymatic hydrolysis or cationic modification. However, previous studies on films (González del Campo et al. 2018; Martín-Sampedro et al. 2022) and foams (Sanguanwong et al. 2021) made of TEMPO CNF and sepiolite also referred an improvement in thermal stability with the addition

of sepiolite to CNFs. For instance, it was recently reported that TEMPO CNF film showed a T_{max} of 297 °C that increased to 307 °C for the composite with 20% sepiolite; the T_{on} was roughly similar in both cases (222–225 °C) (Martín-Sampedro et al. 2022). In the present study, it was used a method of preparation different from that described in the reference above (Martín-Sampedro et al. 2022) to prepare CNF-sepiolite films. Even so, a good thermal stability for TEMPO CNF films with sepiolite was demonstrated, an achievement that should be highlighted in the framework of the present study.

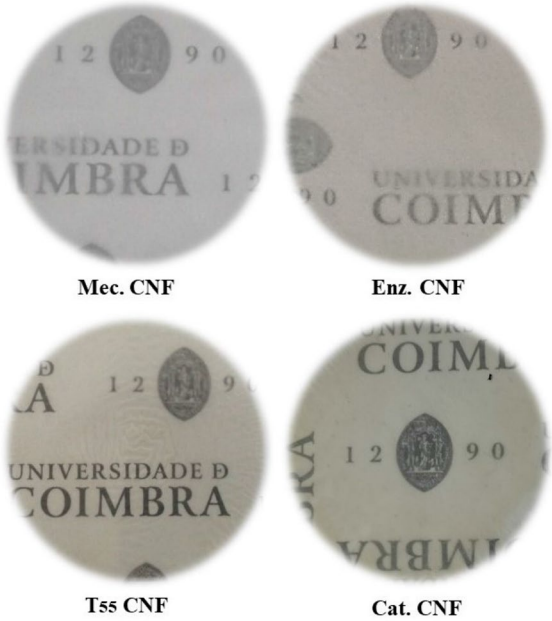

Fig. 4 Digital photographs of the films obtained using the different CNF types

Optical properties of the CNF-based composite films

The transparency of the obtained films was dependent on the type of CNFs used, and, in all cases decreased with the incorporation of the minerals in the composite, as it would be expected (Figs. 4, 5).

The less fibrillated nanocellulose samples, namely Mec CNF and Enz CNF, gave films with lower transparency compared to the samples with higher degrees of fibrillation (Cat CNF and T55 CNF), as expected for neat CNF films. The improved optical properties presented by the films of T55 and Cat CNFs are related to the smaller dimensions of the fibrils, which also allow a more uniform packing, and reduce the dispersion of light by the film, leading to highly transparent materials when no mineral component is used. The further addition of sepiolite in the composite matrix, alone or combined with kaolinite, decreased the transparency since this mineral is an opaque and coloured material, which leads, therefore, to a higher light dispersion/absorption. It should

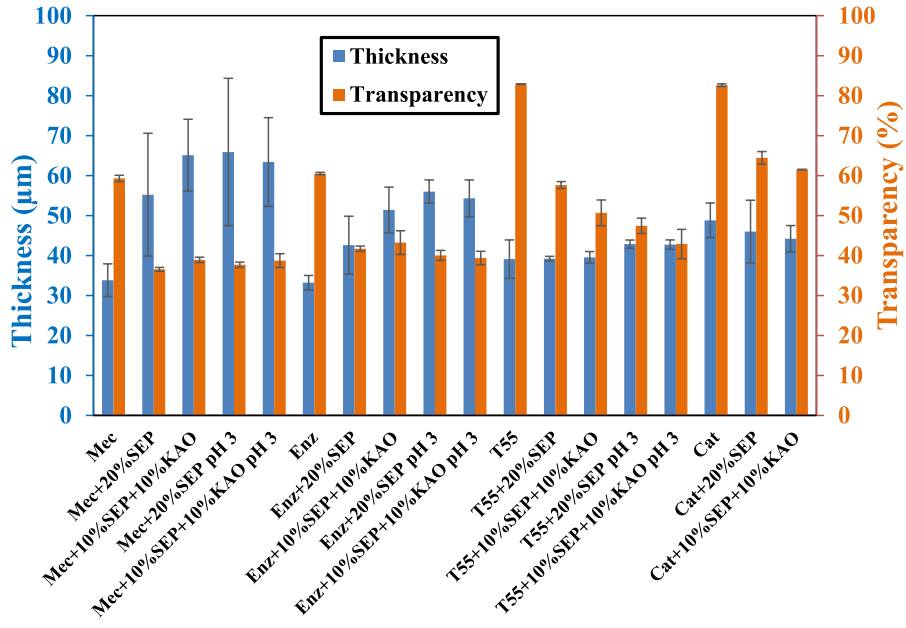

Fig. 5 Thickness and transparency of the CNF-based composite films

be noted that for the films prepared with Mec CNF and Enz CNF, the addition of sepiolite also provided a general increase of the film thickness (for the same grammage). The addition of kaolinite was not translated in a trend towards transparency increment; in some cases, the transparency was even slightly lower when comparing composite films with 10% sepiolite + 10% kaolinite with those of 20% sepiolite (see series of T55 CNF and Cat CNF). Changing the suspension (CNF + mineral) pH to 3 did not benefit the transparency of the produced films either.

It is interesting to note that somewhat higher values of transparency were obtained for the composite films with Cat CNF than for the analogous with T55. The reason for this is not clear. However, it could be antecipated that the positive charges on the surface of the cationic CNF allowed for a better cohesion in the composite film by favoring interaction with the negatively charged particles of the mineral, thus improving the transparency of the film (less air/film interfaces providing lower light scattering).

The transparency values achieved in the CNF-mineral composite films, at a clay load of 20%, were relatively low for the films having Mec CNF of Enz CNF (around 40%). However, with T55 CNF and Cat CNF, values up to 65% for the films with 20% sepiolite were obtained, which can be viewed as more acceptable results regarding film transparency.

Mechanical properties of the CNF-based composite films

The mechanical properties obtained for the prepared films are presented in Fig. 6.

The way the particles can join and interact has a great impact on the properties of the materials, and thus the packing of the particles and their mixture state also have a deep impact on the mechanical properties of the films prepared. The films prepared with neat Mec CNF and Enz CNF presented excellent mechanical performance in what concerns the tensile strength and Young´s modulus, which could be related with longer and thicker fibres/fibrils present in these samples (degree of fibrillation obtained for Mec and Enz CNFs was less than 20%, Table S1). For films containing only CNFs, the presence of these long and thick fibrils may be beneficial, because the packing of CNFs is not impaired, but for composite films the packing of CNFs and mineral particles will be negatively impacted, being the mechanical properties largely affected by the presence of the mineral particles. Contrary, the films prepared with T55 and Cat CNFs did not face a decrease in these mechanical properties, and could even show an improvement in their performance with the introduction of 20% mineral particles, namely in the tensile strength for the T55-mineral composites. The gain in the performance of the latter films can be attributed to a good

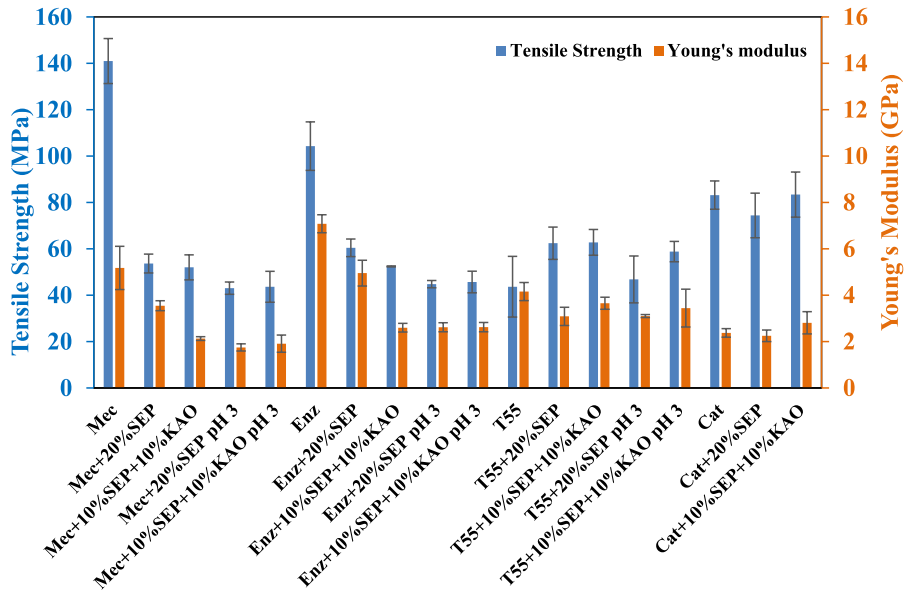

Fig. 6 Mechanical properties of the CNF-based composite films

packing of the mixture of CNFs and mineral particles, established between the thin fibrils of T55 and Cat CNFs and the mineral particles, taking advantage also from the good mechanical properties, i.e., rigidity, of the inorganic particles. The lower degree of fibrillation of Mec CNF and Enz CNF, resulting only in a few thin fibrils did not permit the formation of a compact matrix of CNFs and mineral particles. Chemical interactions through the carboxyl or the alkylammonium functional groups of T55 CNF and Cat CNF, respectively, and the silanol groups of the mineral particles could also favour a higher compatibility between the mineral and CNFs, in comparison to Mec CNF and Enz CNF. The thinner and functionalized T55 and Cat fibrils allow thus a better entanglement with the mineral particles, giving rise to a stronger network and consequently improving the mechanical properties of the resultant composites. Also, it was observed that the more ductile films were the ones prepared with Cat CNF, with an elongation at break near 20% for both the neat CNF film and the CNF composite films (Table S2). Previously reported composite films of nanocelulose with sepiolite showed maximum elongation values of ca. 4% and, in some cases, the elongation was reduced from the neat CNFs to the composite films (González del Campo et al. 2020, 2018; Martín-Sampedro et al. 2022). The present results show that Cat CNF alone or combined with fibrous clay allows for films with a larger elongation at break, not possible with other CNF types.

One of the main difficulties faced to prepare films using T55 and Cat CNFs by filtration + hot pressing is the long dewatering times needed. For samples with low charge density and lower fibrillation degree, as is the case of Mec CNF and Enz CNF, the films can be prepared fastly by filtration + hot pressing due to the fast removal of water from the CNFs or CNF + mineral suspensions. However, for the cases of highly charged and more fibrillated CNFs the water removal time is largely increased (filtration time of ca. 10–30 min for the preparation of films of Mec and Enz CNFs and ca. 1–4 h for the preparation of films of Cat and T55 CNFs, as neat CNF films). A promising strategy to speed up the preparation of films, containing negatively charged fibrils, may be the reduction of the charge density of the CNFs, for example, by decreasing the pH value of the suspensions (Alves et al. 2020a). However, it is crucial to keep the aggregation of the fibrils in a controlled range, avoiding the loss of properties of the films (Alves et al. 2020a). Applying this approach, it was possible to reduce the filtration time of neat T55 film from ca. 4 h to 1h40 min (ca. 2.4 times faster). Additionally, the results shown in Fig. 6 do not evidence a negative impact on the mechanical properties of the composite films with T55, when the suspension pH was reduced to 3 in the preparation of these films (except for a slight decrease in the tensile strength for the case of T55 + sepiolite at pH 3). Therefore, the controlled aggregation of fibrils and fibrils + mineral allowed the arrangement of the particles similar to the dewatering at neutral pH, but with the advantage of reducing the preparation time. This strategy is highly relevant thinking in a scale-up process of film preparation, because the long dewatering times are pointed as one of the main drawbacks in industrial processes employing TEMPO-oxidised CNF (Amini et al. 2019). In a work related to this thematic, Fall et al. (2022) studied the dewatering of several types of CNFs, but considered a different approach to dewater the CNF suspensions, based on a piston press process, which allowed reaching final solid contents of approximately 20–30%. It is important to note that the dewatering rate changes during the entire dewatering process, being higher in the biggening and lower when the water content in the wet cake becomes very low.

Barrier properties of the CNF-based composite films

The barrier properties of composite films are crucial for some applications, such as food packaging, printed electronics or old document restoration. The WVTR and OTR results obtained for the CNF-based composite films are presented in Fig. 7.

In line with the observed mechanical properties of the CNF-based composite films, the oxygen barrier properties of the films prepared using Mec and Enz CNFs were deeply affected by the addition of mineral particles. The neat Mec CNF and Enz CNF films presented good OTR results, ca. 10–20 $cm^3\ m^{-2}\ day^{-1}$, which were fully lost with the addition of sepiolite, being even not possible to measure the OTR values of the films with Mec CNF and minerals (out of the range of the equipment, > 60,000 $cm^3\ m^{-2}\ day^{-1}$). The films containing Enz CNF and minerals were also greatly affected by the addition of sepiolite (OTR increases from ca. 10 $cm^3\ m^{-2}\ day^{-1}$ to more than

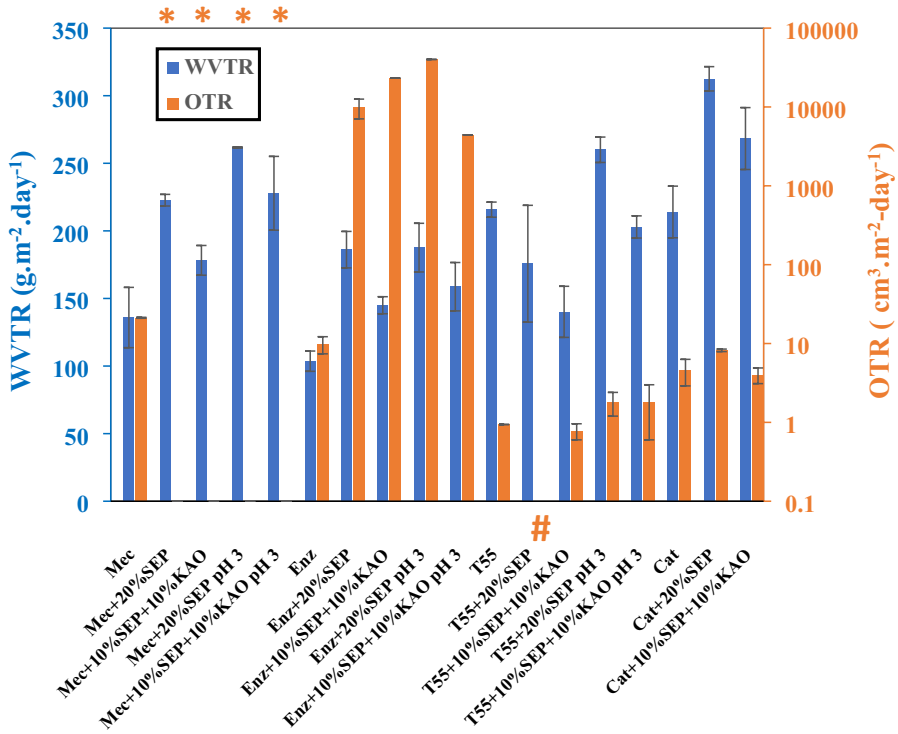

Fig. 7 Water vapour and oxygen barrier properties of the CNF-based composite films. OTR results marked with (*) and (#) mean that the values obtained for the films were out of the range of the equipment, overflow and underflow, respectively

10,000 cm^3 m^{-2} day^{-1}), being the oxygen barrier only slightly recovered by the simultaneous addition of kaolinite and the decrease of the suspension pH value used in the film preparation. On the other hand, the films prepared using T55 and Cat CNFs, as neat or as composites with minerals, presented excellent oxygen barrier properties, below 10 cm^3 m^{-2} day^{-1} for all the prepared films. The best OTR result was obtained for the film prepared using T55 and 20% sepiolite (< 0.4 cm^3 m^{-2} day^{-1}, below the minimum value able to be measured by the equipment-underflow). Also, the composite films of T55 with sepiolite and kaolinite, prepared at near neutral pH or at pH 3, or the composite with sepiolite prepared at pH 3, presented excellent oxygen barrier properties, ≤ 1.8 cm^3 m^{-2} day^{-1}. It is important to note that these values of OTR are better than most of commercial plastics, such as films made of polypropylene and films of polyethylene, which present values of ca. 1000 and 3000 cm^3 m^{-2} day^{-1}, respectively (Manikantan et al. 2022; Soltani and Spontak 2017).

The films using Cat CNF also showed very good oxygen barrier properties, only slightly lower than those of the films employing T55 CNF. These OTR results are in good agreement with the mechanical properties, revealing that a compact matrix of the films formed with more fibrillated CNFs and mineral, can avoid the oxygen molecules diffusion through the films, contrary to the films prepared with low fibrillated CNF samples (Mec and Enz CNFs), which formed films with low compactness and consequently allowing the easy passage of oxygen.

When the oxygen barrier performance is presented in terms of oxygen permeability (OP) values, the same aforementioned trends were observed (Table 3), in account for the fact that the films do not vary substantially from each other regarding film thickness. OP was ≤ 0.1 cm^3 mm m^{-2} day^{-1} atm^{-1} for the T55-based composite films, and ≤ 0.5 cm^3 mm m^{-2} day^{-1} atm^{-1} for the composite films with Cat CNF. For the composite film of T55 and 20% sepiolite, the OP was certainly lower than 0.02 cm^3 mm m^{-2} day^{-1} atm^{-1}. These results confirmed the high oxygen barrier of the composite films prepared with T55 CNF or Cat CNF and the sepiolite mineral, evidenced by the OTR results. Comparing our films with plastics possessing high oxygen barrier, such as ethylene vinyl alcohol (EVOH) or poly(vinylidene chloride) (PVDC), the two plastics with the highest oxygen barrier used in commercial materials, some of our films present

Table 3 Oxygen permeability values of films prepared by filtration + hot pressing with CNFs and minerals (basis weight of 40 g m^{-2})

Film	Oxygen permeability (cm^3 mm m^{-2} day^{-1} atm^{-1})	Water vapour permeability $\times 10^6$ (g m Pa^{-1} day^{-1} m^{-2})
Mec CNF	1.3 ± 0.2	5.9 ± 0.8
Mec CNF + 20% SEP	> 2800	10.4 ± 1.3
Mec CNF + 10% SEP + 10% Kao	> 2800	7.5 ± 0.5
Mec CNF + 20% SEP, pH 3	> 2800	13.3 ± 2.0
Mec CNF + 10% SEP + 10% Kao, pH3	> 2800	11.0 ± 1.1
Enz CNF	0.55 ± 0.14	3.4 ± 0.4
Enz CNF + 20% SEP	536 ± 157	5.4 ± 0.6
Enz CNF + 10% SEP + 10% Kao	1301[a]	5.8 ± 0.4
Enz CNF + 20% SEP, pH 3	2283[a]	8.2 ± 1.0
Enz CNF + 10% SEP + 10% Kao, pH3	248[a]	6.5 ± 1.0
T55 CNF	0.043	6.5 ± 0.3
T55 CNF + 20% SEP	< 0.02	5.4 ± 1.5
T55 CNF + 10% SEP + 10% Kao	0.036 ± 0.008	4.2 ± 0.3
T55 CNF + 20% SEP, pH 3	0.11 ± 0.03	8.6 ± 0.1
T55 CNF + 10% SEP + 10% Kao, pH3	0.089 ± 0.056	6.6 ± 0.1
Cat CNF	0.39 ± 0.08	5.7 ± 0.5
Cat CNF + 20% SEP	0.52 ± 0.13	11.7 ± 0.6
Cat CNF + 10% SEP + 10% Kao	0.33 ± 0.12	8.8 ± 0.4

Measurements were made at 23 °C and 50% RH

[a]Only the determination of one replicate was possible being the other replicate out of the range of the equipment

better barrier properties (in the same RH and temperature measurement conditions). For example, EVOH presents an oxygen permeability value ranging from 0.04 to 0.4 cm^3 mm m^{-2} day^{-1} bar^{-1}, and PVDC ranging from 0.01 to 0.3 cm^3 mm m^{-2} day^{-1} bar^{-1} (Michiels et al. 2017). Our films, such as neat T55 film (0.04 cm^3 mm m^{-2} day^{-1} bar^{-1}), T55 + 20% SEP (< 0.02 cm^3 mm m^{-2} day^{-1} bar^{-1}), T55 + 10% SEP + 10% Kao (0.04 cm^3 mm m^{-2} day^{-1} bar^{-1}) and T55 + 10% SEP + 10% Kao, pH 3 (0.09 cm^3 mm m^{-2} day^{-1} bar^{-1}) generically present better oxygen barrier.

Contrary to OTR, the WVTR of the prepared films did not change so dramatically amongst all samples, being observed WVTR values between ca. 100 and 300 g m^{-2} day^{-1}. The use of highly fibrillated (and functionalized) CNFs did not provide films with an enhanced capacity to avoid water vapour permeation, perhaps due to the presence of hydrophilic counterions which can act as water access points. Even the adjustment of the suspension pH to 3 (while keeping the same formulation composition), did not allow an improved water vapour barrier of the composite films, as higher WVTR values were generally obtained, including in the case of T55 films. Conversely, the addition of a small portion of kaolinite always had a positive impact on the water barrier properties of the films. A WVTR of 140 g m^{-2} day^{-1} was obtained for the film with T55 + 10% sepiolite + 10% kaolinite, which is a good result considering the results reported so far for CNF-mineral composites (most of them higher than 150 g m^{-2} day^{-1}) (González del Campo et al. 2020; Ho et al. 2012; Honorato et al. 2015; Spence et al. 2011).

Thus, some synergistic effects, such as the mixture of a fibrous and a planar mineral, or the use of low pH values, can improve the barrier properties of the composite films, or allow the fast preparation of the materials, and to the best of our knowledge were not explored so far. Overall, as for the oxygen and water vapour barrier properties, the films of T55 + 20% sepiolite and T55 + 10% sepiolite + 10% kaolinite provided the best results. However, if all properties of the films are considered together (namely transparency, tensile strength, elongation at break, oxygen barrier, water vapour barrier, and char residue), besides the two abovementioned films, the Cat + 10% sepiolite + 10% kaolinite film also showed good performance. The film of T55 + 10% sepiolite + 10% kaolinite prepared at pH 3 was also very good in terms

of oxygen barrier and char residue, but it exhibited a very low transparency. The film of Cat CNF + 20% sepiolite although not as good as the other T55- and Cat-based films for the gas barrier, it presented the best transparency and elongation at break of all the prepared composite films. Thus, according to the results obtained in this work, the selection of the film can be tuned to the desired purpose. If the purpose is to obtain an improved water vapour barrier, the lamellar mineral incorporation in the CNF composites adds to the performance. However, for an excellent oxygen barrier, the incorporation of the fibrous mineral in the TEMPO CNF composite is enough. Other properties such as transparency, tensile strength, elongation at break or char residue can be adjusted by an appropriate selection of the composite components and the preparation conditions.

Conclusions

In the present work, four different types of cellulose nanofibres (CNFs) and two clay minerals, single (sepiolite) or combined (sepiolite + kaolinite), were explored in the production of composite films. It was possible to prepare composite films with remarkable oxygen barrier properties (OTR < 0.4 $cm^3\ m^{-2}\ day^{-1}$) using TEMPO-oxidised CNF and 20% sepiolite. Very good oxygen barrier was indeed obtained for all composite films prepared with T55 CNF and Cat CNF (OTR ≤ 1.8 $cm^3\ m^{-2}\ day^{-1}$ and ≤ 8.2 $cm^3\ m^{-2}\ day^{-1}$, respectively). These CNF-based composite films also showed a good mechanical performance, at least similar or even better that that of the neat CNF films. The high oxygen barrier could be explained by the compactness of the films induced by an improved entanglement of the organic (CNFs) and mineral (clay) particles, possible due to the high compatibility between the thin and functionalized fibrils of T55/Cat CNFs and the clay particles. Additionally, the results achieved for the water vapour barrier were acceptable, especially when kaolinite was also added in the composite preparation (WVTR of 140 g $m^{-2}\ day^{-1}$ for the film of T55 + 10% sepiolite + 10% kaolinite). On the other hand, the films prepared using Mec CNF or Enz CNF and sepiolite (or sepiolite + kaolinite) showed poor oxygen barrier, and the mechanical properties of the neat CNF films were highly affected by the addition of the clay minerals. Overall, when all measured properties (mechanical, optical, gas barrier, char residue) are considered together, the films that performed better were the T55 + 20% sepiolite, T55 + 10% sepiolite + 10% kaolinite and Cat + 10% sepiolite + 10% kaolinite.

A decrease in the pH of the suspensions used to prepare the films led to a decrease in film preparation time, without a major negative impact on the composite film properties, leading even to an improvement in the thermal stability. It should be noted, as well, that in the present study the preparation of the films was carried out using high-speed shearing to prepare the sepiolite and sepiolite + CNF suspensions previously to the film formation. This is easier to implement in large scale production than other methods usually employed for dispersion, such as ultrasonication, which may be viewed as an advantage for the present work over other related works.

Acknowledgments The authors would like to acknowledge Fundação para a Ciência e Tecnologia (FCT) and FEDER for the financial support. The CIEPQPF is also acknowledged for the facilities and resource's availability during the project development.

Author contributions Conceptualization—LA and JAFG; Investigation—LA, AR, and JAFG; Methodology—LA, EF; Writing—original draft—LA and JAFG; review and editing—LA, AR, EF, PJTF, MGR and JAFG; Funding acquisition—MGR and JAFG; Project administration—JAFG and PJTF. All authors have read and agreed to the published version of the manuscript.

Funding Open access funding provided by FCT|FCCN (b-on). The present research was supported by the R&D Project "FILCNF-New generation of composite films of cellulose nanofibrils with mineral particles as high strength materials with gas barrier properties" (PTDC/QUI-OUT/31884/2017, CENTRO 01-0145-FEDER-031884) and the Strategic Research Centre Projects UIDB/00102/2020 and UIDB/05488/2020, funded by the Fundação para a Ciência e Tecnologia (FCT) and FEDER.

Data availability All data and materials are available within this article.

Declarations

Conflict of interest The authors declare no competing interests.

Ethics approval and consent to participate No animal experiments or human participant involvement in the study.

Consent for publication All the authors have consented to publish this article in Cellulose, Springer Nature.

References

Abbasi S, Soltani N, Keshavarzi B, Moore F, Turner A, Hassanaghaei M (2018) Microplastics in different tissues of fish and prawn from the Musa Estuary, Persian Gulf. Chemosphere 205:80–87. https://doi.org/10.1016/j.chemosphere.2018.04.076

Almeida RO, Ramos A, Alves L, Potsi E, Ferreira PJT, Carvalho MGVS, Rasteiro MG, Gamelas JAF (2021) Production of nanocellulose gels and films from invasive tree species. Int J Biol Macromol 188:1003–1011. https://doi.org/10.1016/j.ijbiomac.2021.08.015

Alves L, Ferraz E, Gamelas JAF (2019) Composites of nanofibrillated cellulose with clay minerals: a review. Adv Colloid Interface Sci 272:101994. https://doi.org/10.1016/j.cis.2019.101994

Alves L, Ferraz E, Lourenço AF, Ferreira PJT, Rasteiro MG, Gamelas JAF (2020a) Tuning rheology and aggregation behaviour of TEMPO-oxidised cellulose nanofibrils aqueous suspensions by addition of different acids. Carbohydr Polym 237:116109. https://doi.org/10.1016/j.carbpol.2020.116109

Alves L, Ferraz E, Santarén J, Rasteiro MG, Gamelas JAF (2020b) Improving colloidal stability of sepiolite suspensions: effect of the mechanical disperser and chemical dispersant. Minerals 10:779. https://doi.org/10.3390/min10090779

Alves L, Ramos A, Rasteiro MG, Vitorino C, Ferraz E, Ferreira PJT, Puertas ML, Gamelas JAF (2022) Composite films of nanofibrillated cellulose with sepiolite: effect of preparation strategy. Coatings 12:303. https://doi.org/10.3390/coatings12030303

Amini E, Tajvidi M, Bousfield DW, Gardner DJ, Shaler SM (2019) Dewatering behavior of a wood-cellulose nanofibril particulate system. Sci Rep 9:14584. https://doi.org/10.1038/s41598-019-51177-x

Castro DO, Karim Z, Medina L, Häggström JO, Carosio F, Svedberg A, Wågberg L, Söderberg D, Berglund LA (2018) The use of a pilot-scale continuous paper process for fire retardant cellulose-kaolinite nanocomposites. Compos Sci Technol 162:215–224. https://doi.org/10.1016/j.compscitech.2018.04.032

Fall A, Henriksson M, Karppinen A, Opstad A, Heggset EB, Syverud K (2022) The effect of ionic strength and pH on the dewatering rate of cellulose nanofibril dispersions. Cellulose 29:7649–7662. https://doi.org/10.1007/s10570-022-04719-y

Ferraz E, Alves L, Sanguino P, Santarén J, Rasteiro MG, Gamelas JAF (2021) Stabilization of palygorskite aqueous suspensions using bio-based and synthetic polyelectrolytes. Polymers 13:129. https://doi.org/10.3390/polym13010129

Gamelas JAF, Ferraz E (2015) Composite films based on nanocellulose and nanoclay minerals as high strength materials with gas barrier capabilities: key points and challenges. BioResources 10:6310–6313. https://doi.org/10.15376/biores.10.4.6310-6313

Ghanadpour M, Carosio F, Ruda MC, Wågberg L (2018a) Tuning the nanoscale properties of phosphorylated cellulose nanofibril-based thin films to achieve highly fire-protecting coatings for flammable solid materials. ACS Appl Mater Interfaces 10:32543–32555. https://doi.org/10.1021/acsami.8b10309

Ghanadpour M, Wicklein B, Carosio F, Wågberg L (2018b) All-natural and highly flame-resistant freeze-cast foams based on phosphorylated cellulose nanofibrils. Nanoscale 10:4085–4095. https://doi.org/10.1039/C7NR09243A

González del Campo MM, Darder M, Aranda P, Akkari M, Huttel Y, Mayoral A, Bettini J, Ruiz-Hitzky E (2018) Functional hybrid nanopaper by assembling nanofibers of cellulose and sepiolite. Adv Funct Mater 28:1703048. https://doi.org/10.1002/adfm.201703048

González del Campo MM, Caja-Munoz B, Darder M, Aranda P, Vázquez L, Ruiz-Hitzky E (2020) Ultrasound-assisted preparation of nanocomposites based on fibrous clay minerals and nanocellulose from microcrystalline cellulose. Appl Clay Sci 189:105538. https://doi.org/10.1016/j.clay.2020.105538

Gupta P, Verma C, Maji PK (2019) Flame retardant and thermally insulating clay based aerogel facilitated by cellulose nanofibers. J Supercrit Fluids 152:104537. https://doi.org/10.1016/j.supflu.2019.05.005

Hale RC, Seeley ME, La Guardia MJ, Mai L, Zeng EY (2020) A global perspective on microplastics. J Geophys Res Oceans 125:e2018JC014719. https://doi.org/10.1029/2018JC014719

Ho TTT, Zimmermann T, Ohr S, Caseri WR (2012) Composites of cationic nanofibrillated cellulose and layered silicates: water vapor barrier and mechanical properties. ACS Appl Mater Interfaces 4:4832–4840. https://doi.org/10.1021/am3011737

Honorato C, Kumar V, Liu J, Koivula H, Xu C, Toivakka M (2015) Transparent nanocellulose-pigment composite films. J Mater Sci 50:7343–7352. https://doi.org/10.1007/s10853-015-9291-7

Köklükaya O, Carosio F, Durán VL, Wågberg L (2020) Layer-by-layer modified low density cellulose fiber networks: a sustainable and fireproof alternative to petroleum based foams. Carbohydr Polym 230:115616. https://doi.org/10.1016/j.carbpol.2019.115616

Lisuzzo L, Wicklein B, Lo Dico G, Lazzara G, del Real G, Aranda P, Ruiz-Hitzky E (2020) Functional biohybrid

materials based on halloysite, sepiolite and cellulose nanofibers for health applications. Dalton Trans 49:3830–3840. https://doi.org/10.1039/C9DT03804C

Magalhães S, Alves L, Medronho B, Romano A, Rasteiro MDG (2020) Microplastics in ecosystems: from current trends to bio-based removal strategies. Molecules 25:3954. https://doi.org/10.3390/molecules25173954

Manikantan MR, Pandiselvam R, Arumuganathan T, Varadharaju N, Sruthi NU, Mousavi Khaneghah A (2022) Development of linear low-density polyethylene nanocomposite films for storage of sugarcane juice. J Food Process Eng 45:e13988. https://doi.org/10.1111/jfpe.13988

Martín-Sampedro R, Eugenio ME, Ibarra D, Ruiz-Hitzky E, Aranda P, Darder M (2022) Tailoring the properties of nanocellulose-sepiolite hybrid nanopapers by varying the nanocellulose type and clay content. Cellulose 29:5265–5287. https://doi.org/10.1007/s10570-022-04565-y

Michiels Y, Puyvelde PV, Sels B (2017) Barriers and chemistry in a bottle: mechanisms in today's oxygen barriers for tomorrow's materials. Appl Sci 7:665. https://doi.org/10.3390/app7070665

Pedrosa JFS, Rasteiro MG, Neto CP, Ferreira PJT (2022) Effect of cationization pretreatment on the properties of cationic Eucalyptus micro/nanofibrillated cellulose. Int J Biol Macromol 201:468–479. https://doi.org/10.1016/j.ijbiomac.2022.01.068

Sanguanwong A, Flood AE, Ogawa M, Martín-Sampedro R, Darder M, Wicklein B, Aranda P, Ruiz-Hitzky E (2021) Hydrophobic composite foams based on nanocellulose-sepiolite for oil sorption applications. J Hazard Mater 417:126068. https://doi.org/10.1016/j.jhazmat.2021.126068

Soltani I, Spontak RJ (2017) 1—Nanotechnological strategies yielding high-barrier plastic food packaging. In: Grumezescu AM (ed) food packaging. Academic Press, London, pp 1–43

Spence KL, Venditti RA, Rojas OJ, Pawlak JJ, Hubbe MA (2011) Water vapor barrier properties of coated and filled microfibrillated cellulose composite films. BioResources 6:4370–4388. https://doi.org/10.15376/biores.6.4.4370-4388

Wang A, Wang W (2019) 1—Introduction. In: Wang A, Wang W (eds) Nanomaterials from clay minerals. Elsevier, Amsterdam, pp 1–20

Wang J, Gardner DJ, Stark NM, Bousfield DW, Tajvidi M, Cai Z (2018) Moisture and oxygen barrier properties of cellulose nanomaterial-based films. ACS Sustain Chem Eng 6:49–70. https://doi.org/10.1021/acssuschemeng.7b03523

Zeng J, Zeng Z, Cheng Z, Wang Y, Wang X, Wang B, Gao W (2021) Cellulose nanofibrils manufactured by various methods with application as paper strength additives. Sci Rep 11:11918. https://doi.org/10.1038/s41598-021-91420-y